Nd zero-energy scattering

C. R. Chen* and G. L. Payne
Department of Physics and Astronomy, University of Iowa, Iowa City, Iowa 52242

J. L. Friar and B. F. Gibson
Theoretical Division, Los Alamos National Laboratory, Los Alamos, New Mexico 87545

(Received 11 March 1991)

Faddeev-type configuration-space three-body scattering equations are solved for selected two-body- and two-body-plus-three-body-potential model Hamiltonians to obtain absolute predictions for the nucleon-deuteron scattering lengths $^2a_{nd}$, $^4a_{nd}$, $^2a_{pd}$, and $^4a_{pd}$. Convergence for these zero-energy scattering parameters as a function of the number of *NN*-potential partial waves included in the calculation is attained for the first time. Kohn variational estimates provide a measure of the precision of our numerical results. The *nd* predictions agree well with the measured values. The *pd* predictions differ substantially from accepted experimental values which are extrapolated from measurements made above 400 keV.

I. INTRODUCTION

The elastic scattering of nucleons by deuterons at zero incident energy is the simplest three-body scattering problem which nuclear physicists can investigate. Solving the exact few-body equations which describe the three-nucleon system enables one to test our understanding of nuclear forces by direct comparison of model calculations with experimental data [1–7] and to probe for novel features of physical observables [8,9]. Although trinucleon bound-state investigations have yielded interesting examples in each category, it is the scattering problem which provides the better opportunity to explore in depth the accuracy of our knowledge of the nucleon-nucleon (*NN*) interactions. Nonetheless, it was some time after Faddeev's innovative formulation[10] of the three-body scattering problem that the correct set of experimental neutron-deuteron (*nd*) spin-doublet ($^2a_{nd}$) and spin-quartet ($^4a_{nd}$) scattering lengths were discerned from the competing possibilities [11–13] and shown to agree qualitatively with Faddeev calculations using schematic nuclear potentials. It is now clear that the value of the *nd* doublet scattering length is closely correlated with the triton binding energy (E_B), as first suggested by Phillips [14], and that the *nd* quartet scattering length is determined primarily by the properties of the deuteron [15,16]. The situation in the case of proton-deuteron (*pd*) scattering has not been so clear. Phase-shift analyses of the available low-energy *pd* elastic scattering data indicated sizable Coulomb corrections, but Alt's estimate [17] for the *pd* quartet scattering length ($^4a_{pd}$) was significantly larger than the experimental value, as were our subsequent central-force model calculations [9]. Furthermore, our doublet scattering length ($^2a_{pd}$) calculations [9,18] implied values which are in complete disagreement with the quoted experimental estimates [19–21], being smaller than $^2a_{nd}$ rather than larger. However, as discussed below, we believe that this disagreement is now understood.

The generally accepted experimental values for the *nd* scattering lengths are

$$^2a_{nd}=0.65\pm0.04 \text{ fm} ,$$

$$^4a_{nd}=6.35\pm0.02 \text{ fm} .$$

These were determined from elastic scattering of 130 eV neutrons [12]. One can extrapolate to zero energy from much higher energy using the effective-range expansion, but there is a pole in the effective-range function which lies just below threshold [11,22—25]. Therefore, the radius of convergence of the expansion is small, which originally led to some confusion as to proper value for $^2a_{nd}$. The now-established relationship (Phillips line) between the triton binding energy and doublet scattering length supports the validity of the above-quoted experimental numbers, and we demonstrate this quantitatively below for several realistic force models.

The agreement between theory and experiment for the *pd* scattering lengths is not as good. The *pd* scattering data are known less precisely, because the Coulomb barrier greatly suppresses the cross section (much of which is pure Coulomb scattering and therefore uninteresting). In addition, the data exist only for c.m. energies above 400 keV. The (zero-energy) *pd* scattering lengths were obtained by extrapolation from the available (not-so-low-energy) data [19—21]. The reported doublet scattering lengths are

$$^2a_{pd}\begin{cases}1.3\pm0.2 \text{ fm (Ref. [19])}\\ 2.73\pm0.10 \text{ fm (Ref. [20])}\\ 4.00^{+1.00}_{-0.67} \text{ fm (Ref. [21])}\end{cases} .$$

The agreement among the experimental groups is much better for the quartet scattering length. The values cluster around $^4a_{pd}=11.5$ fm. However, Alt's early

separable-potential estimate [17] for $^4a_{pd}$ of 13.3 fm using the (AGS) equations [26] was in clear disagreement. Our own local-potential, central-force estimate [9] of $^4a_{pd}(\simeq 14$ fm) appeared to confirm qualitatively the validity of Alt's estimate. Furthermore, we found $^2a_{pd}\simeq 0$, in obvious disagreement with the above-quoted experimental values and with the established relationship between $^2a_{nd}$ and $B(^3H)$. (Model calculations employing short-range two-body forces show that $^2a_{nd}$ increases as the magnitude of the triton binding decreases.) The zero-energy extrapolation of finite-energy results from a central-force Faddeev calculation by Kvitsinsky [27] disagreed with our zero-energy result and agreed with the experimental data, although additional calculations by other groups [28,29] agreed with our findings. After our $j\leq 1$ tensor-force calculations confirmed our earlier result ($^4a_{pd}$ lies in the range 13.5–14.0 fm and $^2a_{pd}$ is very small) [18], we examined carefully the extrapolation of *pd* scattering to zero energy in a central-force model calculation [30]. Although our calculated phases fell within the existing errors of the data, we found it necessary to have data below 300 keV in order to extrapolate reliably to zero energy. The pole in the *pd* effective range expansion produces such enormous curvature for c.m. energies 300 keV that extrapolation from energies above that value is completely unreliable. Based on this, we believe that we agree with the finite-energy results of Kvitsinsky and Merkuriev [27,31].

The somewhat confused *pd* scattering length situation and the limited scope and validity of the published model results for the *nd* scattering lengths is the motivation for this work. In the latter case three-body forces have only been included in 5-channel ($^2a_{nd}$) and 7-channel ($^4a_{nd}$) calculations (see Sec. II for a discussion of three-body channels), or in perturbation theory. It is now known that three-body-force effects in the triton are nonperturbative and are significant only when higher partial waves are included (i.e., 18- and 34-channel triton models) [3,6]. Furthermore, Efimov [32] as well as Adhikari and coworkers [29,33] have undertaken simple neutron-deuteron effective-interaction representations of the long-range forces that result from the nucleon-exchange mechanism in the three-body scattering process. Valid tests of such effective *Nd* interactions clearly require benchmark calculations in terms of the fundamental short-range *NN* forces in a Faddeev-type formalism.

We report here "complete" *nd* and *pd* scattering length results from calculations carried out within the Faddeev framework which include for the first time all potential partial waves with $j\leq 4$, for several nuclear Hamiltonians that are comprised of contemporary two-body-force and two-body-plus-three-body-force models. Kohn variational estimates [34] are obtained from our configuration-space Faddeev continuum wave functions as a check. The Faddeev partial-wave series converges rapidly. We believe that our estimates of the *nd* and *pd* scattering lengths are converged to within 0.1 fm. Our results therefore provide a benchmark for other calculational techniques. Furthermore, plotting our doublet scattering lengths as a function of the corresponding trinucleon binding energy results in a smooth polynomial fit that permits interpolation of accurate best estimates for $^2a_{nd}$ and $^2a_{pd}$ at the physical trinucleon binding energies.

In the following section we review the three-body scattering equations in configuration space and the required boundary conditions, and we outline the numerical methods employed to solve them. In Sec. III we present numerical results for the potential models that we investigate along with our best estimates of the *nd* and *pd* scattering lengths extrapolated from these studies [35]. Our conclusions are summarized in Sec. IV.

II. CONFIGURATION-SPACE EQUATIONS

Faddeev's innovative work on the three-body continuum problem was inspired by the fact that the Lippmann-Schwinger equation formulation of the three-body scattering problem does not uniquely define the solution [36]. The Faddeev decomposition (or its equivalent) of the scattering amplitude provides a convenient means of enforcing the boundary conditions required to obtain a unique solution. Noyes outlined the configuration-space boundary-condition problem for *nd* scattering [37], and the Grenoble group then developed this approach to the point of obtaining numerical solutions [38]. Including the Coulomb interaction in configuration space for energies below the threshold for breakup of the deuteron is straightforward but nontrivial. Redish [39], Sasakawa and Sawada [40], and Merkuriev [41] have all contributed to solving the Coulomb problem. We utilize the approach adopted in our asymptotic normalization calculations [42]. Our formalism for this problem has been explicated previously for both the bound-state and scattering problems [3,9,18]. We review briefly the essentials.

The three-body equations are solved by making a partial-wave expansion of the *NN* potential and the Faddeev amplitude. Faddeev calculations are traditionally characterized by the number of three-body angular momentum states or channels, where each channel is specified by the quantum numbers of an interacting pair of nucleons and the corresponding quantum numbers of the remaining spectator nucleon. For a total angular momentum equal to 1/2 there are two such channels for each *NN* interacting pair partial wave, except for the case in which the *NN* total angular momentum (j) is 0 (where the number of channels is restricted to 1). A common approximation is to solve the doublet Faddeev equations when only five channels are included, which corresponds to retaining only the dominant $(^1S_0, ^3S_1 — ^3D_1)$ *NN*-potential partial waves or, alternatively, all even-parity *NN* partial waves with $j\leq 1$. The 9-channel truncation corresponds to retaining only the even-parity *NN* partial waves with $j\leq 2$. When all *NN* partial waves with $j\leq 2$ are retained, one has the 18-channel solution. The 34-channel solution corresponds to retaining all *NN* partial waves with $j\leq 4$. In our bound-state investigations, we demonstrated that 34-channel solutions had converged to within ~ 10 keV of the full model answer [43]. That is, the higher $(4<j\leq 8)$ partial waves of two contemporary force models were shown to contribute 10 keV to the triton binding energy (out of roughly 8 MeV), and the convergence of the binding energy with respect to the num-

ber of *NN* partial waves was shown to be roughly geometrical due to the angular momentum barrier. For total trinucleon angular momentum equal to 3/2, the number of three-body channels is considerably larger than for 1/2. Solutions for all even-parity *NN* partial waves with $j \leq 1$ correspond to seven channels. Retaining all even-parity *NN* partial waves with $j \leq 2$ implies 15 channels. The solution for all *NN* partial waves with $j \leq 2$ requires 30 channels, and the solution retaining all *NN* partial waves with $j \leq 4$ has 62 channels.

To find the *Nd* scattering lengths we solve the configuration-space Faddeev equations for the case of zero-energy incident nucleons, and then we read the scattering length from the asymptotic solution for the Faddeev amplitude. The Faddeev amplitudes are defined by decomposing the total wave function Ψ into a sum of the three Faddeev amplitudes

$$\Psi=\Psi_1(\mathbf{x}_1,\mathbf{y}_1)+\Psi_2(\mathbf{x}_2,\mathbf{y}_2)+\Psi_3(\mathbf{x}_3,\mathbf{y}_3) , \tag{1}$$

where $\mathbf{x}_i$ and $\mathbf{y}_i$ are the Jacobi coordinates

$$\mathbf{x}_i=\mathbf{r}_j-\mathbf{r}_k \tag{2a}$$

and

$$\mathbf{y}_i=\tfrac{1}{2}(\mathbf{r}_j+\mathbf{r}_k)-\mathbf{r}_i \tag{2b}$$

for three nucleons with coordinates $\mathbf{r}_1$, $\mathbf{r}_2$, and $\mathbf{r}_3$. The values of i, j, and k are cyclic. The Schrödinger equation

$$\left[T+\sum_i V(\mathbf{x}_i)+\sum_i V_C(x_i)-E\right]\Psi=0 \tag{3}$$

can be decomposed into the three coupled Faddeev equations

$$[T+V(\mathbf{x}_i)+V_C(x_1)+V_C(x_2)+V_C(x_3)-E]\Psi_i(\mathbf{x}_i,\mathbf{y}_i) = -\mathbf{V}(\mathbf{x}_i)[\Psi_j(\mathbf{x}_j,\mathbf{y}_j)+\Psi_k(\mathbf{x}_k,\mathbf{y}_k)] , \tag{4}$$

where T is the kinetic-energy operator, $\mathbf{V}(\mathbf{x}_i)$ is the short-range nuclear interaction, and

$$V_C(x_i)=\frac{e^2}{x_i}\frac{[1+\tau_z(j)][1+\tau_z(k)]}{4} \tag{5}$$

is the two-body Coulomb potential. We have retained the entire Coulomb potential on the left-hand side of Eq. (4) so that the long-range Coulomb distortion is present in each Faddeev amplitude. This greatly facilitates the implementation of the boundary conditions [41,42]. In addition, we have found that this procedure is more stable for our numerical calculations.

For three identical nucleons all three Faddeev amplitudes will have the same functional form, and it is only necessary to solve one of the three Faddeev equations. To solve the first Faddeev equation we use the j-J coupling scheme and write Ψ_1 in the form

$$\Psi_1(\mathbf{x}_1,\mathbf{y}_1)=\sum_\alpha \frac{\psi_\alpha(x_1,y_1)}{x_1 y_1}|\alpha\rangle , \tag{6}$$

where

$$|\alpha\rangle=|[(l_\alpha,s_\alpha)j_\alpha,\ (L_\alpha,S_\alpha)J_\alpha]\mathcal{J}\mathcal{M};\ (t_\alpha,T_\alpha)\mathcal{T}\mathcal{M}_T\rangle , \tag{7}$$

l_α is the relative orbital angular momentum of particles 2 and 3, s_α is the spin angular momentum of particles 2 and 3, j_α is the total angular momentum of particles 2 and 3, L_α is the orbital angular momentum of particle 1 relative to the center of mass of particles 2 and 3, S_α is the spin of particle 1($S_\alpha=\frac{1}{2}$), J_α is the total angular momentum of particle 1, $\mathcal{J}$ is the total angular momentum ($\mathcal{J}=\frac{1}{2},\frac{3}{2}$), t_α is the isospin of particles 2 and 3, T_α is the isospin of particle 1, and $\mathcal{T}$ is the total isospin ($T_\alpha=\mathcal{T}=\frac{1}{2}$), which we will assume to be conserved. The tiny isospin impurity in *pd* scattering is known to be unimportant [9].

We obtain a set of coupled partial differential equations for the reduced channel amplitudes $\psi_\alpha(x_1,y_1)$ by substituting the expansion of Ψ_1, into the first Faddeev equation and then projecting the equation on each channel by taking the inner product with each of the $|\alpha\rangle$. Multiplying each equation by $-x_1y_1M/\hbar^2$, and transforming to the hyperspherical variables defined by

$$x_1=\rho\cos\theta \tag{8a}$$

and

$$y_1=(\sqrt{3}/2)\rho\sin\theta , \tag{8b}$$

we obtain the set of equations

$$(\Delta_\alpha-\kappa^2)\psi_\alpha(\rho,\theta)-\sum_{\alpha'}(v_{\alpha\alpha'}+v^C_{\alpha\alpha'})\psi_{\alpha'}(\rho,\theta) = \sum_{\alpha''}v_{\alpha\alpha''}\sum_{\alpha'}\int_{\theta^-}^{\theta^+}d\theta' K_{\alpha''\alpha'}(\theta,\theta')\psi_{\alpha'}(\rho,\theta') , \tag{9}$$

where we have defined

$$v_{\alpha\alpha'}=\frac{M}{\hbar^2}\langle\alpha|V(\mathbf{x}_1)|\alpha'\rangle , \tag{10a}$$

$$v^C_{\alpha\alpha'}=\frac{M}{\hbar^2}\langle\alpha|V_C(x_1)+V_C(x_2)+V_C(x_3)|\alpha'\rangle , \tag{10b}$$

$$\sum_{\alpha'}\int_{\theta^-}^{\theta^+}d\theta' K_{\alpha''\alpha'}(\theta,\theta')\psi_{\alpha'}(\rho,\theta') = x_1y_1[\alpha''|\Psi_2\rangle+\langle\alpha''|\Psi_3\rangle], \tag{10c}$$

$$E=-\frac{\hbar^2\kappa^2}{M} , \tag{10d}$$

and

$$\Delta_\alpha=\frac{\partial^2}{\partial\rho^2}+\frac{1}{\rho}\frac{\partial}{\partial\rho}+\frac{1}{\rho^2}\frac{\partial}{\partial\theta^2}-\frac{l_\alpha(l_\alpha+1)}{\rho^2\cos^2\theta}-\frac{L_\alpha(L_\alpha+1)}{\rho^2\sin^2\theta} . \tag{10e}$$

The integration limits θ^- and θ^+ are the same as for the bound-state calculations [3], and for zero-energy scattering κ is the two-body bound-state (deuteron) wave number.

Next we express the channel function as the sum of the known incident partial wave and the unknown scattered wave $\Omega_\alpha(x_1,y_1)$:

$$\psi_\alpha(x_1,y_1)=\phi_\alpha(x_1,y_1)+\Omega_\alpha(x_1,y_1) , \tag{11}$$

where ϕ_α is the incident reduced wave. For the incident s wave, we have

$$\phi_\alpha(x_1,y_1)=y_1\mathcal{J}(z)u_d(x_1)\ . \tag{12}$$

Here $u_d(x_1)$ is the reduced deuteron bound-state wave function and $\mathcal{J}(z)$ can be expressed in terms of a modified Bessel function of order 1:

$$\mathcal{J}(z)=z^{-1/2}I_1(2\sqrt{z})\ . \tag{13}$$

The quantity $z=2\alpha\mu y_1$ in the argument depends upon the fine structure constant α and the reduced mass μ of the nucleon-deuteron system.

Inserting Eq. (11) into Eq. (9) one obtains the following equation for the reduced scattering function Ω_α:

$$(\Delta_\alpha-\kappa^2)\Omega_\alpha(\rho,\theta)-\sum_{\alpha'}(v_{\alpha\alpha'}+v^C_{\alpha\alpha'})\Omega_{\alpha'}(\rho,\theta)-\sum_{\alpha''}v_{\alpha\alpha''}\sum_{\alpha'}\int_{\theta^-}^{\theta^+}d\theta' K_{\alpha''\alpha'}(\theta,\theta')\Omega_{\alpha'}(\rho,\theta')$$
$$=\sum_{\alpha'}(v^C_{\alpha\alpha'}-\omega\delta_{\alpha\alpha'})\phi_{\alpha'}(\rho,\theta)+\sum_{\alpha''}v_{\alpha\alpha''}\sum_{\alpha'}\int_{\theta^-}^{\theta^+}d\theta' K_{\alpha''\alpha'}(\theta,\theta')\phi_{\alpha'}(\rho,\theta')\ , \tag{14}$$

where

$$\omega=\frac{M}{\hbar^2}\frac{e^2}{y_1}\ . \tag{15}$$

For large values of y_1 the outgoing wave Ω_α has the asymptotic form

$$\Omega_\alpha(x_1,y_1)\underset{y_1\to\infty}{\to}-a_\alpha\mathcal{K}_\alpha(y_1)u_d(x_1) \tag{16}$$

for the deuteron channels, where

$$\mathcal{K}_\alpha(z)=\frac{(2\alpha\mu)^{L_\alpha}}{(2L_\alpha)!}(2\sqrt{z})K_{2L_\alpha+1}(2\sqrt{z}) \tag{17}$$

and $K_{2L_\alpha+1}$ is the modified Bessel function. The quantity a_α in Eq. (16) is the scattering length extracted from our numerical solution.

For the closed channels the function Ω_α approaches zero in the asymptotic region. In order to simplify the numerical calculations we express Ω_α in terms of the smoother auxiliary function F_α, which is defined by

$$\Omega_\alpha(x_1,y_1)=F_\alpha(\rho,\theta)[y_1^{L_\alpha}\mathcal{K}_\alpha(y_1)]\frac{u_d(x_1)}{x_1} \tag{18a}$$

for the deuteron channels and

$$\Omega_\alpha(x_1,y_1)=F_\alpha(\rho,\theta)e^{-\kappa\rho} \tag{18b}$$

for the remaining channels. In Eq. (18a) we have included the factor $y_1^{L_\alpha}$ to remove the singular behavior of $\mathcal{K}_\alpha(y_1)$ at $y_1=0$. In addition, we have included the factor of $1/x_1$ in Eq. (18a) to simplify the boundary conditions at $x_1=0$.

Because Ω_α is the reduced wave function, the boundary conditions for $F_\alpha(\rho,\theta)$ are

$$F_\alpha(0,\theta)=F_\alpha(\rho,0)=F_\alpha(\rho,\pi/2)=0 \tag{19}$$

for all channels,

$$F_\alpha(\rho,\theta)\underset{y_1\to\infty}{\to}a_\alpha\frac{x_1}{y_1^{L_\alpha}}=A(\theta)\rho^{1-L_\alpha} \tag{20a}$$

for the deuteron channels, and

$$F_\alpha(\rho,\theta)\underset{\rho\to\infty}{\to}\text{constant} \tag{20b}$$

for the nondeuteron channels. These boundary conditions are implemented by requiring that at $\rho=\rho_{\max}$

$$\frac{\partial F_\alpha}{\partial\rho}=\frac{(1-L_\alpha)}{\rho}F_\alpha \tag{21a}$$

for the deuteron channels, and

$$\frac{\partial F_\alpha}{\partial\rho}=0 \tag{21b}$$

for the nondeuteron channels.

Substituting the expression for Ω_α given in Eq. (18) into Eq. (14) yields a set of coupled differential equations for the $F_\alpha(\rho,\theta)$. To solve these equations we use a bicubic spline expansion

$$F_\alpha(\rho,\theta)=\sum_{i,j}a_{ij}^\alpha s_i(\rho)s_j(\theta)\ , \tag{22}$$

where the spline functions were chosen to be the cubic Hermite splines [44]. We use the orthogonal collocation method to solve for the unknown coefficients a_{ij}^α. This method consists of writing each of the channel equations in Eq. (14) at N collocation points (ρ_1,θ_m), where N is equal to the number of unknowns, a_{ij}^α. For the cubic Hermite splines the collocation points are chosen to be the two Gauss quadrature points in each interval for the ρ splines and in each interval for the θ splines. If we choose 15 intervals for the ρ variable (i.e., $N_\rho=16$) and 15 intervals for the θ variable ($N_\theta=16$), then we get $30\times30=900$ equations for each channel. Each equation will contain all of the unknown a_{ij}^α for all of the channels used in the expansion in Eq. (6). Thus, if we have N_c channels and each channel has N unknown spline coefficients a_{ij}^α, we have a set of $N_c\times N$ simultaneous linear equations to solve. These equations can be written as the matrix equation

$$(A-B)x=b\ , \tag{23}$$

where the matrix A comes from the first two terms in Eq. (14) and the matrix B is the third term on the left-hand side of Eq. (14). The column matrix x contains the un-

known a_{ij}^{α} and the column matrix b is the right-hand side of Eq. (14).

In our previous scattering calculations [9,18] which were limited to at most seven channels, we simply solved this matrix equation. For the calculations presented in this paper we have used up to 62 channels, and the direct solution of Eq. (22) becomes prohibitive in terms of the computer time. Thus we have used an iterative method to solve the matrix equation. The matrix A is a block diagonal matrix while the matrix B is a full matrix. One procedure that generates an iterative solution for Eq. (22) is to rewrite the matrix equation in the form

$$Ax = b + Bx \tag{24a}$$

or

$$x = A^{-1}b + A^{-1}Bx \ . \tag{24b}$$

However, we found that iterating this equation was numerically unstable for some cases. Hence, we used a different procedure which consists of rewriting Eq. (22) in the form

$$(1 - BA^{-1})Ax = b \ . \tag{25}$$

Now, if we let

$$BA^{-1} = H \tag{26}$$

and

$$Ax = y \ , \tag{27}$$

then we get the equation

$$y = b + Hy \ , \tag{28}$$

which can be solved by an iterative technique for y. Once we have found y, we can solve Eq. (27) for x.

One means of solving Eq. (28) is to use the Padé method [see Ref. (45)]. In this approach one introduces the parameter λ in Eq. (28)

$$y = b + \lambda Hy \ , \tag{29}$$

which is then iterated to give the series

$$y = b + \lambda Hb + \lambda^2 H^2 b + \cdots \ , \tag{30}$$

and this series is summed by using Padé approximants. We found that this method could be used for the Argonne potential but was numerically unstable for configuration-space calculations with the Reid potential, which has a stronger repulsive core. Consequently, we had to employ a different method of solution. We found that the Lanczos method [46], which we have used for our bound-state calculation, could be used to obtain stable accurate results. However, this requires solving both the matrix equation and its transpose equation, which doubles the computer time required. Therefore we finally solved Eq. (28) by generating a series of basis vectors using a Gram-Schmidt procedure instead of the Lanczos method.

We start with the vector

$$y_0 = b \ , \tag{31}$$

and generate the vector

$$\tilde{y}_1 = Hb \ . \tag{32}$$

Then the vector y_1 is written as

$$y_1 = c_0 y_0 + c_1 \tilde{y}_1 \ , \tag{33}$$

where the constants c_0 and c_1 are determined by the conditions

$$y_0^T y_1 = 0 \tag{34a}$$

and

$$y_1^T y_1 = 1 \ . \tag{34b}$$

In general, given the vectors $y_1, y_2, \ldots, y_n$, the vector $\tilde{y}_{n+1}$ is generated by

$$\tilde{y}_{n+1} = Hy_n \ , \tag{35}$$

and then the vector y_{n+1} is expressed as

$$y_{n+1} = \sum_{i=0}^{n} c_i y_i + c_{n+1}\tilde{y}_{n+1} \ , \tag{36}$$

where the constants c_i, $i = 1, 2, \ldots, n+1$, are determined from the conditions

$$y_i^T y_{n+1} = 0 \quad i = 1, 2 \ldots, n \tag{37a}$$

and

$$y_{n+1}^T y_{n+1} = 1 \ . \tag{37b}$$

Given the set of basis vectors y_i, the approximate solution to Eq. (28) can be written as

$$y = \sum_{i=1}^{n} a_i y_i \ . \tag{38}$$

The constants a_i are determined by substituting the expansion in Eq. (38) into Eq. (28) and rewriting it as

$$(1 - H)\sum_i a_i y_i = b \ . \tag{39}$$

Taking the inner product with y_j, we have

$$a_j + \sum_{i=1}^{n} y_j^T H y_i a_i = y_j^T b \ , \tag{40}$$

and this set of n equations can be solved for a_i. The number of basis vectors y_i is increased until a stable result is obtained.

Some care was required in choosing the collocation points. Although we are dealing with short-range forces, we must still integrate the differential equations to large distances (~ 60 fm), where the influence of the permuted elastic terms [the right-hand side of Eq. (4)] is negligible.

In addition, care is required to make the density of points high along the strip where the outgoing deuteron resides.

To check the accuracy of our solution, we used the numerical wave function in a Kohn [34] variational procedure for the scattering length. When the Kohn result agreed with the asymptotic value of the scattering length to the desired accuracy, then the solution was judged to be converged. Both a channel-projected result, in which the Coulomb potential was projected so that the Kohn estimate corresponded directly to that of the Faddeev solution, and a full-(Coulomb) potential result were calculated. These differed when the Coulomb potential was included in the *pd* case and served as a measure of the missing Coulomb strength due to our truncation of the two-body interacting-pair partial waves. For the doublet calculation, the difference occurred in the third significant figure of the scattering length.

III. NUMERICAL RESULTS

The parameters which we vary to ensure an accurate solution are the numbers and distribution of the ρ_l and θ_m points and the value of $\rho_{\max}$ beyond which we assume that the wave function has achieved its asymptotic form. The ρ breakpoints can be distributed uniformly between the origin and a small radius of 0.5–1.0 fm ($\rho^I_{\rm br}$) if the interaction is strongly repulsive. From that breakpoint out to 12–14 fm ($\rho^M_{\rm br}$) they are distributed with a nonuniform spacing using a scale factor, S_ρ: $\rho_{n+1}-\rho_n=S_\rho(\rho_n-\rho_{n-1})$. Between that point and $\rho_{\max}$, the breakpoints are again distributed uniformly. If the scale factor is chosen so that the ρ breakpoints are not too closely spaced, then the first region can be omitted. The θ breakpoints were distributed uniformly between 0 and $\pi/6$ (N^I_θ) and between $\pi/6$ and $\pi/3$(N^M_θ), and they were scaled by S_θ between $\pi/3$ and $\pi/2$ (N^E_θ) in order to ensure that a sufficient number was concentrated in the region where the wave function has the most structure. Selected cases are listed in Table I.

Kohn variational checks were invaluable in determining an optimum mesh. We quote below values of the scattering lengths a_{nd} and a_{pd} along with the Kohn variational estimates a^K_{nd} and a^K_{pd} based upon the Faddeev amplitude and the channel-projected interaction (short range and Coulomb). Comparison of these results provides the correct consistency check. In the *pd* case we also quote results for $a^{K,F}_{pd}$, Kohn variational results without the channel projection of the Coulomb interaction. That is, $a^{K,F}_{pd}$ includes all the higher partial waves of the long-range Coulomb potential. It is $a^{K,F}_{pd}$ which provides the best estimate of the physical *pd* scattering length.

We have limited our investigation to two different *NN* potential modes and two different two-pion-exchange three-body-force models. Specifically, we have used the Reid soft-core (RSC) two-body force [47] (having a very stiff repulsive core) alone and in combination with the somewhat singular Tucson-Melbourne (TM) three-nucleon force [48]. For comparison we have also used the Argonne V_{14} (AV14) two-body force [49] (having a relatively soft repulsive core) alone and in combination with the less singular Brazilian (BR) three-nucleon force [50]. The RSC spin-singlet force was fitted to *pp* scattering data while that of the AV14 was fitted to *np* scattering data. This largely accounts for their 300 keV difference in binding energy [3–7,51,52]. In both cases we know that the two-body-force model underbinds the triton while the two-body-plus-three-body-force model overbinds the triton (for a πN cutoff Λ in the two-pion-exchange three-nucleon force of $5.8m_\pi$;$m_\pi=139.6$ MeV).

In Table II we list results for the RSC model for *nd* and *pd* doublet (quartet) scattering lengths in the 3-channel (2-channel) approximation for selected mesh parameters shown in Table I. Because three-body-force effects are small for these limited numbers of three-body channels, we restrict this comparison to a two-body force. The Kohn variational estimates provide a feel for the accuracy of each solution when compared to the results obtained from the Faddeev wave function. It is clear from this initial study that $\rho_{\max}=64.0$ fm is a reasonable cutoff. Also, S_ρ and $S_\theta\sim1.5$ are reasonable choices. For $S_\rho\sim1.5$, one need not divide the ρ variable into three regions; indeed, in most of the calculations discussed below we scaled the region (0,14.0) fm. A θ distribution of (12,2,1) provides satisfactory results, but we use (12,3,2) below for the three-body-force models, because they induce more structure in the wave function.

In Tables III and IV we list results for all four model

TABLE I. Selected sets of mesh parameters used to test accuracy and convergence of the RSC and RSC/TM model calculations.

Case	$(\rho^I_{\rm br},\rho^M_{\rm br},\rho_{\max})$	$(N^I_\rho,N^M_\rho,N^E_\rho)$	S_ρ	$(N^I_\theta,N^M_\theta,N^E_\theta)$	S_θ
1	(0.5,12.0,50.0)	(5,10,6)	1.2	(12,4,2)	1.35
2	(0.5,12.0,50.0)	(5,10,6)	1.5	(12,4,2)	1.5
3	(0.5,12.0,50.0)	(5,10,6)	1.6	(12,4,2)	1.6
4	(0.0,14.0,54.0)	(0,13,4)	1.5	(12,3,2)	1.5
5	(0.0,14.0,64.0)	(0,13,5)	1.5	(12,3,2)	1.5
6	(0.0,14.0,74.0)	(0,13,6)	1.5	(12,3,2)	1.5
7	(0.0,14.0,84.0)	(0,13,7)	1.5	(12,3,2)	1.5
8	(0,0,14.0,94.0)	(0,13,8)	1.5	(12,3,2)	1.5
9	(0.0,14.0,54.0)	(0,13,4)	1.6	(12,3,2)	1.5
10	(0.0,14.0,64.0)	(0,12,5)	1.5	(12,3,2)	1.5
11	(0.0,14.0,64.0)	(0,13,5)	1.5	(12,2,1)	1.5

TABLE II. RSC *Nd* 3-channel (doublet) and 2-channel (quartet) scattering length results for mesh parameters listed in Table I. Units are fm.

Case	$^2a_{nd}$	$^2a_{nd}^K$	$^2a_{pd}$	$^2a_{pd}^K$	$^4a_{nd}$	$^4a_{nd}^K$	$^4a_{pd}$	$^4a_{pd}^K$
1	1.819	2.363						
2	2.360	2.346						
3	2.378	2.355						
4	2.356	2.346						
5	2.353	2.350	3.442	3.449				
6	2.353	2.349	3.437	3.446				
7	2.353	2.349	3.437	3.446				
8	2.353	2.349	3.437	3.446				
9	2.359	2.354	3.455	3.457				
10	2.351	2.351	3.472	3.466	6.309	6.305	13.375	13.337
11	2.350	2.351	3.461	3.465	6.304	6.305	13.362	13.338

Hamiltonians based upon the following mesh parameters: $\rho_{bk}=(0.0,14.0,64.0)$ and $N_\rho=(0,13,5)$ with $S_\rho=1.5$; $N_\theta=(12,2,1)$ with $S_\theta=1.5$ for the NN force alone and $N_\theta=(12,3,2)$ otherwise. The column N_c defines the number of three-body channels in the calculation. The variation of $^2a_{nd}$ and $^2a_{pd}$ with N_c corresponds to similar variations seen for the trinucleon binding energies—neither are monotonic functions of N_c. The fact that a_{Nd}^K does not bound a_{Nd} reflects the fact that the Kohn variational principle produces a stationary value, not a bound as variational principles produce for the ground state. The significant variation of $^2a_{Nd}$ with N_c reflects the strong correlation of scattering length with trinucleon binding energy—the Phillips line for $^2a_{nd}$ and $B(^3H)$. The lack of variation in $^4a_{Nd}$ with N_c reflects the fact that the quartet scattering length is determined principally by the properties of the deuteron, which are fully present in the $N_c=2$ calculations. Note that $^2a_{pd}$, $^2a_{pd}^K \rightarrow {}^2a_{pd}^{K,F}$, and $^4a_{pd}$, $^4a_{pd}^K \rightarrow {}^4a_{pd}^{K,F}$ as N_c increases. That is, the Coulomb interaction is included more completely as N_c is increased. Finally, the spread in the last digits of the quartet calculations is an indication of the precision in our calculations. That is, we do not believe the final digits are significant, but we include them in the tables so that one can understand the convergence of our computations.

In the case of the doublet scattering lengths, it is possible to plot $^2a_{Nd}$ vs E_B and interpolate by means of a smooth curve to determine the values of the scattering lengths which correspond to the physical binding energy. Alternatively, one can adjust the three-body-force cutoff Λ so that the trinucleon binding energies have their experimental values (8.48 and 7.72 MeV) and then ask for the values of scattering lengths for those Hamiltonians. We collect the results of such calculations in Table V.

We summarize our spin-doublet results in Fig. 1.

TABLE III. *Nd* doublet scattering length results along with Kohn variational estimates and full Kohn *pd* estimates as a function of the number of three-body channels. Units are fm.

N_c	Model	$^2a_{nd}$	$^2a_{nd}^K$	$^2a_{pd}$	$^2a_{pd}^K$	$^2a_{pd}^{K,F}$
5	RSC	1.778	1.774	2.244	2.250	2.102
9		1.610	1.601	1.929	1.931	1.756
18		1.612	1.609	1.741	1.755	1.764
34		1.520	1.519	1.569	1.581	1.582
5	RSC/TM	1.357	1.349	1.402	1.381	1.225
9		0.704	0.691	0.243	0.236	0.043
18		0.309	0.293	−0.655	−0.663	−0.649
34		0.393	0.383	−0.509	−0.505	−0.504
5	AV14	1.364	1.359	1.434	1.432	1.276
9		1.240	1.235	1.231	1.229	1.044
18		1.274	1.275	1.096	1.093	1.105
34		1.200	1.204	0.967	0.965	0.965
5	AV14/BR	0.635	0.648	0.118	0.140	0.031
9		−0.196	−0.191	−1.198	−1.191	−1.408
18		0.092	0.093	−0.994	−0.992	−0.977
34		0.001	−0.001	−1.133	−1.136	−1.136

TABLE IV. *Nd* quartet scattering length results along with Kohn variational estimates and full Kohn *pd* estimates as a function of the number of three-body channels. Units are fm.

N_c	Model	${}^4a_{nd}$	${}^4a_{nd}^K$	${}^4a_{pd}$	${}^4a_{pd}^K$	${}^4a_{pd}^{K,F}$
2	RSC	6.304	6.303	13.362	13.338	13.529
7		6.303	6.303	13.341	13.314	13.528
15		6.299	6.300	13.296	13.264	13.517
30		6.302	6.301	13.563	13.549	13.520
62		6.302	6.304	13.550	13.527	13.521
2	RSC/TM	6.310	6.306	13.376	13.338	13.529
7		6.309	6.305	13.353	13.315	13.528
15		6.305	6.301	13.306	13.265	13.516
30		6.308	6.304	13.588	13.550	13.521
62		6.308	6.304	13.568	13.529	13.522
2	AV14	6.374	6.380	13.563	13.570	13.673
7		6.373	6.378	13.540	13.546	13.762
15		6.370	6.375	13.489	13.496	13.751
30		6.370	6.381	13.782	13.791	13.762
62		6.372	6.380	13.764	13.771	13.764
2	AV14/BR	6.377	6.380	13.565	13.572	13.764
7		6.377	6.378	13.558	13.565	13.759
15		6.720	6.376	13.491	13.498	13.752
30		6.380	6.380	13.785	13.792	13.763
62		6.378	6.381	13.764	13.771	13.765

Scattering lengths are plotted as a function of the binding energy of the corresponding trinucleon bound state for both the *nd* and *pd* systems. In each case we include results from all four models. We emphasize that, by including a three-body force and more than five channels in the doublet calculation or more than seven channels in the quartet calculation, we do not have to artificially increase the strength of the *NN* singlet interaction to obtain triton binding energies greater than the experimental datum, in order to extend our Phillips line (for ${}^2a_{nd}$ vs E_B) into the region of overbinding as was done in Refs. [9] and [18]. Our three-body-force calculations here are also much more realistic, because the three-body force becomes much more effective once p waves are allowed in the system (18 and 34 channels).

The ${}^2a_{nd}$ results fall essentially on a straight line (the Phillips line) for all four model calculations. Circles specify RSC values and squares specify AV14 values. The solid symbols indicate 34-channel results. The *nd* datum falls squarely on the line and agrees with the model results for which we adjusted the three-nucleon-force cutoff parameter Λ to give the physical triton binding energy (8.48 MeV). Our best estimates for the *nd* doublet scattering length for the models considered are (with the quoted uncertainties being subjective estimates)

$${}^2a_{nd}=0.57\pm0.01 \text{ fm (AV14}-\text{AV14/BR)},$$

$${}^2a_{nd}=0.66\pm0.01 \text{ fm (RSC}-\text{RSC/TM)}.$$

TABLE V. *Nd* scattering length results for two-body-plus-three-body-force models adjusted to yield the correct trinucleon binding energies. Units are fm. $N_c=34$ for doublet results and $N_c=30$ for quartet results.

Model	${}^2a_{nd}^K$	${}^2a_{pd}^K$	${}^4a_{nd}^K$	${}^4a_{pd}^{K,f}$
RSC/TM	0.657	0.080	6.304	13.521
AV14/BR	0.567	0.068	6.380	13.763

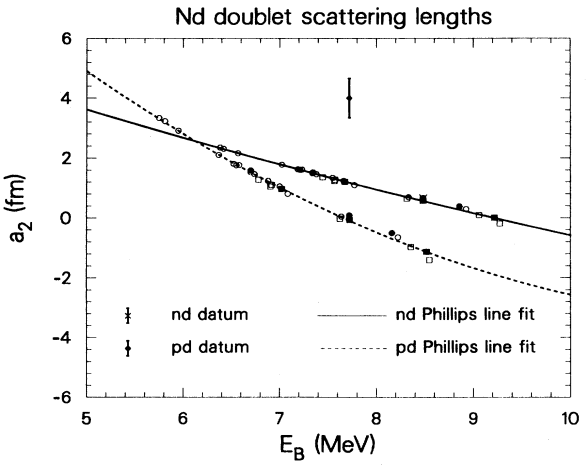

FIG. 1. Neutron-deuteron and proton-deuteron scattering lengths plotted as a function of the corresponding trinucleon binding energy. The circles specify RSC results and the squares specify AV14 results; solid symbols denote 34-channel results. The ${}^2a_{nd}$ datum coincides with the RSC/TM model result for which the three-body force was adjusted to yield the experimental ^{3}H binding. The ${}^2a_{pd}$ datum falls well off the theoretical curve; see text for explanation.

The RSC model nominally agrees better with the data, but the difference between these two numbers best reflects the model dependence of the calculation.

The *pd* calculations map out a parabolic curve, reflecting the effect of an additional scale parameter which is purely Coulombic. The RSC and RSC/TM model results fall slightly above the corresponding AV14 and AV14/BR results. This reflects the slightly greater effect of Coulomb repulsion in the latter models, which exhibit less short-range repulsion—the two protons can come closer to one another. Here the datum lies far off the theoretical curve and far from the two points (${}^2a_{pd} \approx 0$) for which the three-nucleon-force parameter was adjusted to obtain the physical ^{3}He binding energy (7.72 MeV). However, as indicated above and in Ref. [30], we believe that this disagreement is the result of one's inability to extrapolate to zero energy from incident energies above 400 keV due to the strong curvature in the effective-range function below 300 keV.

Our spin-quartet results are displayed in Fig. 2. We plot *nd* results versus *pd* results. Again circles specify RSC and squares specify AV14; solid symbols indicate 62-channel results. We obtain two clusters of predictions, one for the RSC model calculations and one for the AV14 model calculations. Because the Pauli repulsion for three nucleons in the same spin state keeps the nucleons apart, three-body-force effects and the influence of higher *NN* partial waves are minimal. We find for the AV14-AV14/BR model

$$ {}^4a_{nd} = 6.38 \pm 0.01 \text{ fm} , $$

$$ {}^4a_{pd} = 13.76 \pm 0.05 \text{ fm} , $$

while for the RSC-RSC/TM model we find

$$ {}^4a_{nd} = 6.30 \pm 0.01 \text{ fm} , $$

$$ {}^4a_{pd} = 13.52 \pm 0.05 \text{ fm} . $$

The quoted theoretical errors are subjective and merely reflect the spread of points as a function of the number of channels. The RSC value again normally agrees better with the experimental value of ${}^4a_{nd}$. However, we believe that the difference is best construed as a measure of the *NN*-force model dependence for such calculations. The ${}^4a_{pd}$ values differ substantially from the experimental value, but ${}^2a_{pd}$ and ${}^4a_{pd}$ are strongly correlated and the cross sections are difficult to separate. A reduction in the estimate for ${}^2a_{pd}$ (as indicated by our calculations) would likely produce an increase in ${}^4a_{pd}$.

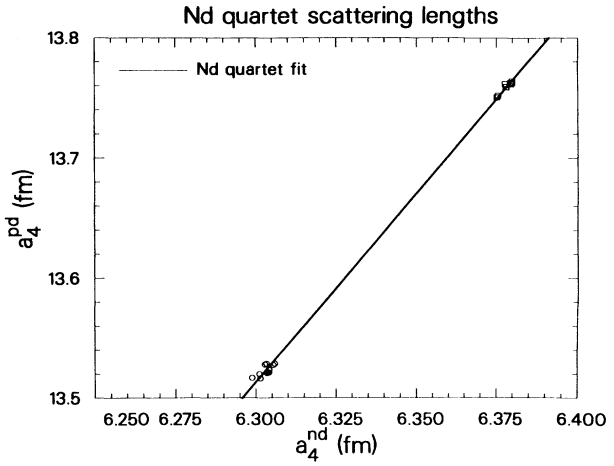

FIG. 2. Neutron-deuteron quartet scattering length plotted vs proton-deuteron quartet scattering lengths. The circles specify RSC results and the squares specify AV14 results; solid symbols denote 62-channel results.

IV. CONCLUSIONS

In summary, we have produced the first absolute predictions for the *nd* and *pd* zero-energy scattering lengths in a Faddeev-type, configuration-space calculation which is converged as a function of the number of *NN*-potential partial waves that are included. Three-body-force effects do not move the doublet scattering length results off the previously deduced (*nd*) Phillips line or *pd* doublet curve. Our *nd* scattering lengths agree well with the published experimental values. Our ${}^2a_{pd}$ estimate (approximately zero) is smaller than ${}^2a_{nd}$, contrary to intuition based upon our experience with short-range forces and to what the Phillips line would therefore naively indicate (an increase in repulsion produces a lower triton binding energy and therefore a larger doublet scattering length). Our ${}^2a_{pd}$ prediction disagrees strongly with experimental values quoted in the literature, but this is likely due to one's inability to extrapolate to zero energy from above 300 keV (c.m.). Our ${}^4a_{pd}$ estimate (13.5–13.8 fm) also disagrees with published experimental results, but this is correlated with the ${}^2a_{pd}$ disagreement. Although low-energy *pd* elastic scattering experiments are difficult, one would hope that these absolute predictions might inspire further efforts in this area.

ACKNOWLEDGMENTS

The work of J.L.F. and B.F.G. was performed under the auspices of the U.S. Department of Energy. That of C.R.C. and G.L.P. was supported in part by the U.S. Department of Energy.

*Present address: Department of Physics, Texas A&M University, College Station, TX.

[1] See I. R. Afnan and J. M. Read, Phys. Rev. C **12**, 293 (1975) and I. R. Afnan and N. D. Birrell, *ibid.* **16**, 823 (1977) for early separable expansion solutions involving realistic local potentials.

[2] J. Chauvin, C. Gignoux, J. J. Benayoun, and A. Laverne, Phys. Lett. **78B**, 5 (1978).

[3] G. L. Payne, J. L. Friar, B. F. Gibson, and I. R. Afnan, Phys. Rev. C **22**, 823 (1980); C. R. Chen, G. L. Payne, J. L. Friar, and B. F. Gibson, *ibid.* **31**, 2366 (1985), compare results of many of the then available calculations; J. L. Friar, B. F. Gibson, and G. L. Payne, *ibid.* **37**, 2869 (1988), compare results for three contemporary one-boson-exchange, momentum-dependent potential models; J. L. Friar, B. F. Gibson, and G. L. Payne, *ibid.* **35**, 1502 (1987), treat Coulomb effects in detail.

[4] C. Hajduk and P. U. Sauer, Nucl. Phys. **A369**, 321 (1981); P. U. Sauer, Prog. Nucl. Phys. **16**, 35 (1986).

[5] A. Bömelburg, Phys. Rev. C **28**, 403 (1983).

[6] S. Ishikawa, T. Sasakawa, T. Sawada, and T. Ueda, Phys. Rev. Lett. **53**, 1877 (1984); T. Sasakawa and S. Ishikawa, Few-Body Syst. **1**, 3 (1986).

[7] K. T. Kim, Y. E. Kim, D. J. Klepacki, R. A. Brandenburg, E. P. Harper, and R. Machleidt, Phys. Rev. C **38**, 2366 (1988).

[8] B. F. Gibson and G. J. Stephenson, Jr., Phys. Rev. C **8**, 1222 (1973); **11**, 1448 (1975).

[9] J. L. Friar, B. F. Gibson, and G. L. Payne, Phys. Lett. **24B**, 287 (1983); Phys. Rev. C **28**, 983 (1983).

[10] L. D. Faddeev, Zh. Eksp. Teor. Fiz. **39**, 1459 (1960) [Sov. Phys. JETP **12**, 1014 (1961)]; see also A. N. Mitra, Nucl. Phys. **32**, 529 (1962) for separable potential equations for the *nd* scattering lengths.

[11] W. T. H. van Oers and J. D. Seagrave, Phys. Lett. **24B**, 562 (1967).

[12] W. Dilg, L. Koester, and W. Nistler, Phys. Lett. **36B**, 208 (1971).

[13] P. Stoler, N. N. Kaushal, F. Green, E. Harms, and L. Laroze, Phys. Rev. Lett. **29**, 1745 (1972); P. Stoler, N. N. Kaushal, and F. Green, Phys. Rev. C **8**, 1539 (1973).

[14] A. C. Phillips, Rep. Prog. Phys. **40**, 905 (1977); Phys. Lett. **28B**, 378 (1969).

[15] A. C. Phillips, Phys. Rev. **142**, 984 (1966); see also A. C. Phillips and G. Barton, Phys. Lett. **28B**, 378 (1969).

[16] G. L. Payne, J. L. Friar, and B. F. Gibson, Phys. Rev. C **26**, 1385 (1982).

[17] E. O. Alt, in *Proceedings of the VII International Conference on Few Body Problems in Nuclear and Particle Physics,* edited by A. N. Mitra, I. Slaus, V. S. Bashin, and V. K. Gupta (North-Holland, Amsterdam, 1976), p. 76.

[18] C. R. Chen, G. L. Payne, J. L. Friar, and B. F. Gibson, Phys. Rev. C **33**, 401 (1986); J. L. Friar, B. F. Gibson, G. L. Payne, and C. R. Chen, *ibid.* **30**, 1121 (1984).

[19] W. T. H. van Oers and K. W. Brockman, Jr., Nucl. Phys. A **92**, 561 (1967).

[20] J. Arvieux, Nucl. Phys. A **221**, 253 (1974).

[21] E. Huttel, W. Arnold, H. Baumgart, H. Berg, and G. Clausnitzer, Nucl. Phys. **A406**, 443 (1983); E. Huttel, W. Arnold, H. Berg, H. H. Kranse, J. Ulbricht, and G. Clausnitzer, *ibid.* **406**, 435 (1986).

[22] R. S. Christian and J. L. Gammel, Phys. Rev. **91**, 100 (1953).

[23] L. M. Delves, Phys. Rev. **118**, 1318 (1961).

[24] A. S. Reiner, Phys. Lett. **28B**, 387 (1969).

[25] J. S. Whiting and M. G. Fuda, Phys. Rev. C **14**, 18 (1976).

[26] E. O. Alt, P. Grassberger, and W. Sandhas, Nucl. Phys. **B2**, 167 (1967).

[27] A. A. Kvitsinsky, Pis'ma Zh. Eksp. Teor. Fiz. **36**, 375 (1982) [JETP Lett. **36**, 455 (1982)].

[28] H. Zankel and L. Mathelitsh, Phys. Lett. **132B**, 27 (1983); G. H. Berthold and H. Zankel, Phys. Rev. **34**, 1203 (1986).

[29] L. Tomio, A. Delfino, and S. K. Adhikari, Phys. Rev. C **35**, 441 (1987).

[30] C. R. Chen, G. L. Payne, J. L. Friar, and B. F. Gibson, Phys. Rev. C **39**, 1261 (1989).

[31] A. A. Kvitsinsky and S. P. Merkuriev, Yad. Fiz. **41**, 647 (1985) [Sov. J. Nucl. Phys. **41**, 412 (1985)].

[32] V. Efimov, Nucl. Phys. **A362**, 45 (1981); **378**, 581(E) (1982); V. Efimov and E. G. Tkachenko, Few-Body Systems **4**, 71 (1988).

[33] S. K. Adhikari, Phys. Rev. C **30**, 31 (1984); S. K. Adhikari and T. K. Das, *ibid.* **37**, 1376 (1988).

[34] W. Kohn, Phys. Rev. **74**, 1763 (1948); J. Nuttal, Phys. Rev. Lett. **19**, 473 (1967); S. P. Merkuriev, Nucl. Phys. **A283**, 395 (1974); for further references, see R. J. Nesbet, *Variational Methods in Electron-Atom Scattering* (Plenum, New York, 1980).

[35] A summary of our best estimates was reported earlier in J. L. Friar, B. F. Gibson, G. L. Payne, and C. R. Chen, Phys. Lett. B **247**, 197 (1990).

[36] L. L. Foldy and W. Tobocman, Phys. Rev. **105**, 1099 (1957).

[37] H. P. Noyes, in *Three Body Problem in Nuclear and Particle Physics,* edited by J. S. C. McKee and P. M. Rolph (North-Holland, Amsterdam, 1970), p. 2.

[38] J. J. Benayoun and C. Gignoux, Nucl. Phys. **A190**, 419 (1972); A. Laverne and C. Gignoux, *ibid.* **203**, 597 (1973); S. P. Merkuriev, C. Gignoux, and A. Laverne, Ann. Phys. (N.Y.) **99**, 30 (1976).

[39] E. F. Redish, in *Few Body System and Nuclear Forces II, Lecture Notes in Physics,* edited by H. Zingl, M. Haftel, and H. Zankel (Springer, Berlin, 1978), Vol. 87, p. 427.

[40] T. Sasakawa and T. Sawada, Phys. Rev. C **20**, 1954 (1979).

[41] S. P. Merkuriev, Yad. Fiz. **23**, 6 (1976) [Sov. J. Nucl. Phys. **23**, 141 (1976)].

[42] J. L. Friar, B. F. Gibson, D. R. Lehman, and G. L. Payne, Phys. Rev. C **25**, 1616 (1982).

[43] J. L. Friar, B. F. Gibson, and G. L. Payne, Phys. Rev. C **36**, 1138 (1987).

[44] P. M. Prenter, *Splines and Variational Methods* (Wiley, New York, 1975).

[45] W. Glöckle, *The Quantum Mechanical Few-Body Problem* (Springer, Heidelberg, New York, 1983).

[46] C. Lanczos, J. Res. Natl. Bureau Stand. **49**, 33 (1952).

[47] R. V. Reid, Ann. Phys. (NY) **50**, 441 (1968); see B. Day, Phys. Rev. C **24**, 1203 (1981) for the higher partial waves.

[48] S. A. Coon, M. D. Scadron, P. C. McNamee, B. R. Barrett, D. W. E. Blatt, and B. H. J. McKellar, Nucl. Phys. A **317**, 242 (1979); S. A. Coon and W. Glöckle, Phys. Rev. C **23**, 1790 (1981).

[49] R. B. Wiringa, R. A. Smith, and T. A. Ainsworth, Phys. Rev. C **29**, 1207 (1984).

[50] H. T. Coelho, T. K. Das, and M. R. Robilotta, Phys. Rev. C **28**, 1812 (1983); M. R. Robilotta and M. P. Isidro, Nucl. Phys. **A414**, 394 (1984); M. R. Robilotta, M. P. Isidro, H. T. Coelho, and T. K. Das, Phys. Rev. C **31**, 646 (1985).

[51] J. L. Friar, B. F. Gibson, and G. L. Payne, Phys. Rev. C **36**, 1140 (1987).

[52] R. A. Brandenburg, P. U. Sauer, and R. Machleidt, Z. Phys. A **280**, 93 (1977).